Role of IL-18 in Second-Hand Smoke–Induced Emphysema

Adelheid Kratzer[1], Jonas Salys[1], Claudia Nold-Petry[2], Carlyne Cool[1], Martin Zamora[1], Russ Bowler[3], Andreas Rembert Koczulla[4], Sabina Janciauskiene[5], Michael G. Edwards[1], Charles A. Dinarello[2], and Laimute Taraseviciene-Stewart[1]

[1]Division of Pulmonary Sciences and Critical Care Medicine, and [2]Division of Infectious Diseases, Department of Medicine, University of Colorado at Denver, Aurora, Colorado; [3]National Jewish Health, Denver, Colorado; [4]Department of Medicine, University Clinic of Giessen and Marburg, Marburg, Germany; and [5]Department of Respiratory Medicine, Hannover Medical School, Hannover, Germany

Chronic second-hand smoke (SHS) exposure comprises the main risk factor for nonsmokers to develop chronic obstructive pulmonary disease (COPD). However, the mechanisms behind the chronic inflammation and lung destruction remain incompletely understood. In this study, we show that chronic exposure of Sprague-Dawley rats to SHS results in a significant increase of proinflammatory cytokine IL-18 and chemokine (C-C motif) ligand 5 in the bronchoalveolar lavage fluid (BALF) and a significant decrease of vascular endothelial growth factor (VEGF) in the lung tissue. SHS exposure resulted in progressive alveolar airspace enlargement, cell death, pulmonary vessel loss, vessel muscularization, collagen deposition, and right ventricular hypertrophy. Alveolar macrophages displayed a foamy phenotype and a decreased expression of the natural inhibitor of IL-18, namely, IL-18 binding protein (IL-18BP). Moreover, IL-18 down-regulated the expression of VEGF receptor–1 and VEGFR receptor–2, and induced apoptosis in pulmonary microvascular endothelial cells *in vitro*. We also observed a trend toward increased concentrations of IL-18 in the BALF of patients with COPD. Our findings suggest that IL-18–mediated endothelial cell death may contribute to vascular destruction and disappearance in SHS-induced COPD. Moreover, IL-18 and IL-18BP are potential new targets for therapeutics.

Keywords: second-hand cigarette smoke; emphysema; inflammation; macrophages; vasculature

Cigarette smoke exposure is the key initiator of chronic inflammation in the lung and a major environmental risk factor in the development of chronic obstructive pulmonary disease (COPD) (1, 2). Although corticosteroids, bronchodilators, and antibiotics relieve the symptoms of COPD, the most effective treatments appear to involve smoking cessation and oxygen supplementation (3). Exposure to second-hand smoke (SHS) comprises the main risk factor for nonsmokers to develop COPD/emphysema in the Western world, whereas worldwide, exposure to biomass smoke is the main cause of COPD in nonsmokers (3). Whereas smokers inhale first-hand smoke directly, SHS is passively inhaled by others and is referred to as environmental tobacco smoke. The two types of smoke have basically the same composition, except that in SHS, toxic products are more concentrated and potentially more hazardous to human health. A recent study showed that in 2004, 0.1% of worldwide mortality was attributable to SHS (4). Even advanced ventilation systems do not eliminate the health hazards in the smoking environment. The mechanism by which SHS or first-hand smoke causes the development of COPD/emphysema remains unknown.

Tobacco smoke affects both innate and adaptive immunity (5), and it has long been proposed that human diseases associated with cigarette smoke may reflect an effect on the immune system (5). Here, we hypothesize that long-term SHS exposure leads to an impairment of immune responses, which in turn leads to the development of COPD/emphysema. We tested our hypothesis in an animal model by exposing Sprague-Dawley (SD) rats to SHS. Our data demonstrate that long-term (2–4 months) SHS exposure leads to significant lung destruction, cell death, and the development of emphysema, and that proinflammatory cytokine IL-18 plays a crucial role in the disappearance of the vasculature.

CLINICAL RELEVANCE

Our results highlight an important role for IL-18 in a second hand smoke–induced lung injury as a contributor to endothelial cell death, leading to the rarefaction of pulmonary vasculature and emphysema. Targeting IL-18–mediated pathways may hold therapeutic potential to treat chronic obstructive pulmonary disease.

MATERIALS AND METHODS

Animals and SHS Exposure

Animal studies were approved by the Institutional Animal Care and Use Committee at National Jewish Health (Denver, CO). Six-week-old male SD rats ($n = 8$/group) (Harlan, Indianapolis, IN) were exposed to SHS 6 hours per day, with a 2-hour resting period. A mixture of sidestream smoke (89%) and mainstream smoke (11%) was produced in a smoking machine (Teague Enterprises, Davis, CA) by smoking five Kentucky 1R3F reference cigarettes (Tobacco Research Institute, University of Kentucky, Lexington, KY) every 9 minutes. The control group was kept in a filtered room-air (RA) environment. The total particulate matter (TPM) concentrations in the chamber were 100–120 $\mu g/m^3$.

IL-18 knockout (KO) mice (C57BL/6 background) and wild-type C57BL/6 mice were obtained from Jackson Laboratory (Bar Harbor, ME). Heat-inactivated *Staphylococcus epidermidis* (100 μl) was instilled intratracheally (6).

(*Received in original form May 11, 2012 and in final form January 2, 2013*)

This study was supported by Flight Attendant Medical Research Institute grant 072053, American Heart Association grants 0735388N and 11 GRNT 7520020, National Institutes of Health grant AI 15614 (C.A.D.), the Emphysema Research Fund, and the Bixler COPD Foundation.

Author Contributions: L.T.-S. and A.K. were responsible for the concept and design of this study. A.K., J.S., C.N.-P., C.C., R.B., and C.A.D. were responsible for the acquisition, analysis, and interpretation of data. A.R.K. and S.J. were responsible for sample acquisition. M.G.E. was responsible for the statistical analysis. A.K., M.Z., C.A.D., and L.T.-S. were responsible for drafting the manuscript in terms of important intellectual content.

Claudia Nold-Petry is currently at the Ritchie Centre, Monash Institute of Medical Research, Clayton, Victoria, Australia.

Correspondence and requests for reprints should be addressed to Laimute Taraseviciene-Stewart, Ph.D., Division of Pulmonary Sciences and Critical Care Medicine, Department of Medicine, University of Colorado at Denver, Anschutz Medical Campus, 12700 E. 19th Ave., 9th Floor, RC-2, Box 272, Aurora, CO 80045. E-mail: Laima.Taraseviciene@ucdenver.edu

This article has an online supplement, which is accessible from this issue's table of contents at www.atsjournals.org

Am J Respir Cell Mol Biol Vol 48, Iss. 6, pp 725–732, Jun 2013

Originally Published in Press as DOI: 10.1165/rcmb.2012-0173OC on February 7, 2013
Internet address: www.atsjournals.org

Tissue Processing and Lung Morphology

The right lungs were ligated and excised for lymphocyte, protein, and RNA isolation. The left lungs were inflated with 0.5% agarose (7), and morphological changes were evaluated according to the recommendations for methods of quantification in the American Thoracic Society guidelines (8, 9). The mean linear intercept (MLI) was determined using automated image analyzer software (special plug-in for Image J; National Institutes of Health, Bethesda, MD) (10–12).

Second-Harmonic Generation Microscopy

The autofluorescence of elastin in the lung tissue was visualized by two-photon excitation (TPE) microscopy, and the autofluorescence of collagen was visualized by second-harmonic generation (SHG) microscopy, using a Zeiss Axiovert 200 with a 510-Meta confocal module and Coherent Chameleon Ultra II as a laser source (Zeiss, Jena, Germany).

Western Blot Analysis, Quantitative PCR, Immunohistochemistry, and Cell Death Assay

Western blot analysis and immunohistochemical staining were performed as described elsewhere (13). Apoptosis was determined using a terminal deoxynucleotidyl transferase dUTP nick end labeling (TUNEL) kit (Roche Applied Science, Mannheim, Germany).

RNA was isolated using an Omega Bio-Tek RNA isolation kit (Life Science Products, Frederick, CO). DNA contamination was eliminated with a DNase I (Invitrogen, Carlsbad, CA) treatment step. The reverse transcription was performed using an ABI high-capacity RT kit (Foster City, CA). Primers were designed for the coding sequences using software from Integrated DNA Technologies (Skokie, IL). Relative quantitative PCR was performed using a 7300 ABI machine.

Bronchoalveolar Lavage Fluid

Bronchoalveolar lavage fluid (BALF) was obtained by collecting two 3-ml instillations of modified Hanks' balanced salt solution. BALF cells underwent Wright-Giemsa staining for morphology.

Cytokine Measurements

Cytokines were measured using a Luminex Rat Cytokine Multiplex-23 Bead Array Assay kit on a Luminex 200 instrument (BioRad, Hercules, CA), and were analyzed with MilliPlex software (Millipore, Billerica, MA). Human IL-18 was measured by ELISA (MBL International, Woburn, MA).

Cells and Cigarette Smoke Extract Preparation

The rat alveolar macrophage (rAM) cell line (CRL-2192) was purchased from the American Type Culture Collection (Manassas, VA).

Rat pulmonary microvascular endothelial cells (RPMVECs) were obtained from the Center of Cell Biology at the University of South Alabama (Mobile, AL).

Cigarette smoke extract (CSE) was prepared as described by Carp and Janoff (14).

Permeability and Migration Assays

Endothelial monolayer (i.e., RPMVECs) permeability was determined using an Evans blue assay. The macrophage migration assay was performed using carboxyfluorescein diacetate succinimidyl ester–labeled rAMs.

Statistical Analysis

Statistical analysis was performed using GraphPad Prism (San Diego, CA) and the Student *t* test or two-way ANOVA. Correlations were determined using one-tailed Pearson correlation. $P < 0.05$ was considered significant.

Detailed methods are provided in the online supplement.

RESULTS

Second-Hand Cigarette Smoke Exposure Leads to Weight Loss, Emphysema, and Cardiac Hypertrophy

The TPM concentrations in the smoking chamber were 100–120 $\mu g/m^3$, mimicking TPM concentrations in smoking casinos and smoking lounges at airports (range, 18.5–205 $\mu g/m^3$) in North America (15, 16). Compared with filtered RA-exposed control animals (Figure 1A), the exposure to SHS resulted in progressive alveolar airspace enlargement (after 2 months of exposure, Figure 1B; after 4 months of exposure, Figure 1C). MLI measurements (Figure 1D) showed a significant difference between RA-exposed (83 ± 1.3 μm) control rat lungs and rat lungs 2 months (102 ± 1.9 μm) and 4 months (132 ± 2.2 μm) after SHS exposure. The complete measurements of emphysematous changes are presented in Table E1 in the online supplement. Right heart hypertrophy was also detectable. The ratio of right ventricle to left ventricle plus septum was significantly increased after 2 months (Figure 1E) and 4 months (Figure 1F) of SHS exposure, indicating the development of mild pulmonary hypertension.

The SD rats showed a significant loss of body weight that was first recorded after 2 weeks of SHS exposure (Figures 1G–1I). Reduced body weight is consistent with the significantly reduced concentrations of leptin (Figure E1 in the online supplement) in the lung tissue. Moreover, SHS exposure dramatically changed the rats' fur color (Figure E2).

SHS Exposure Caused Lung Fibrosis and Cell Death

Imaging of lung sections using SHG with TPE microscopy revealed fibrotic tissue. The autofluorescent images of RA-exposed (Figure 2A), and SHS-exposed (Figure 2B) rat lung tissue showed a significant collagen (red) deposition in SHS-exposed lungs, as quantified in Figure 2C, and less elastic tissue (green).

Cigarette smoke–induced DNA damage was visualized with TUNEL staining. Compared with RA-exposed rat lungs (Figure 2D), a significantly higher number of TUNEL-positive airway epithelial and vascular endothelial cells was evident in the lung tissue after 2 months of SHS exposure (Figure 2E), indicating cell death. The quantitative analysis of the fluorescent intensity of TUNEL staining, measured in relative fluorescence units, is shown in Figure 2F.

Lung Tissue Remodeling and Vascular Endothelial Growth Factor

There was a progressive decrease in vascular endothelial growth factor (VEGF) concentrations in the SHS-exposed rat lung tissue (Figure 2G). Compared with RA-exposed rat lungs (Figure 2H), a significant muscularization of pulmonary blood vessels was detected in rat lungs after 2 months of SHS exposure (Figure 2I), as shown by immunohistochemical analysis. The quantitative analysis of α–smooth muscle actin staining (Figure 2 H and I) is presented in Figure 2J. Concurrently, the number of blood vessels in the SHS-exposed rat lungs was decreased by almost 25% (Figure 2K).

Morphological Changes in Alveolar Macrophages and Cytokines

Staining for the macrophage marker CD68 revealed that lung macrophages in normal tissue were located in close proximity to the airways (Figures 3A and 3B). Conversely, in the SHS-exposed lung tissue, macrophages were detected in the alveolar airspaces (Figures 3C and 3D), and displayed a foamy/spongy phenotype characteristic of the foamy cells observed in atherosclerotic plaques.

Cells in BALF (Figures E3A and E3B) were mainly macrophages (99%). Interestingly, the total cell counts and protein concentrations in the BALF of SHS-exposed rats were lower (Figures E3C–E3E) when compared with RA-exposed control rats.

Immunohistochemical staining for IL-18 showed that in comparison with RA-exposed control rats, significantly higher

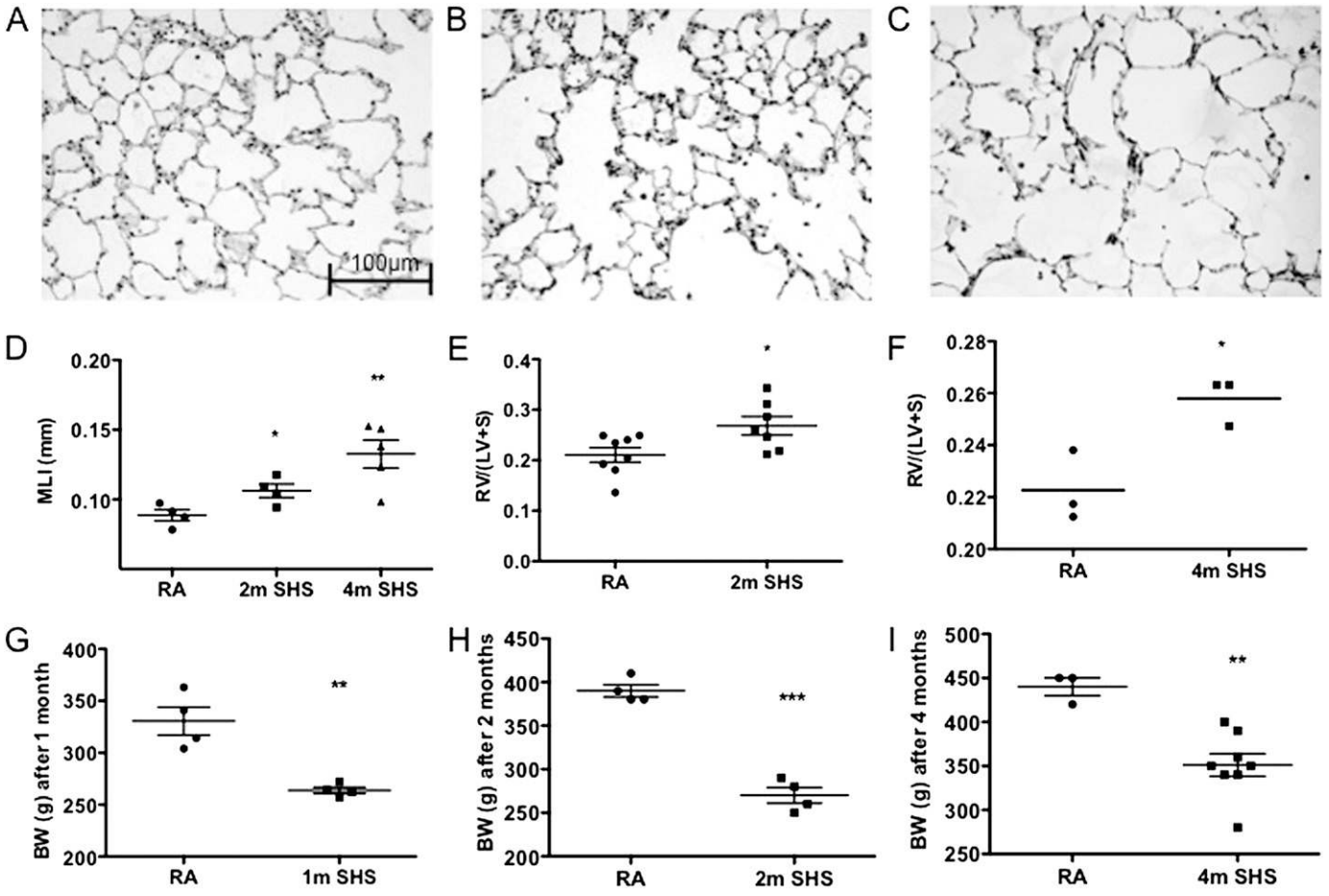

Figure 1. Second-hand smoke (SHS) exposure of 6-week-old male Sprague-Dawley rats ($n = 4$–8 rats/group) leads to emphysematous changes in the lungs and right heart hypertrophy. (*A*–*C*) The histology of hematoxylin and eosin–stained, paraffin-embedded lung tissue sections. (*A*) Room-air (RA) control. (*B*) Two months of SHS exposure. (*C*) Four months of SHS exposure. (*D*) Mean linear intercept (MLI) measurements. Right ventricular hypertrophy was determined by measuring the ratio of right ventricle versus left ventricle plus septum (RV/LV + S) weights after 2 months of SHS exposure (*E*) and 4 months of SHS exposure (*F*). (*G*) Body weight after 1 month of SHS exposure versus RA-exposed control mice. (*H*) Body weight after 2 months of SHS exposure versus RA-exposed control mice. (*I*) Body weight after 4 months of SHS exposure versus RA-exposed control mice. *$P \leq 0.05$. **$P < 0.01$. ***$P < 0.001$. BW, body weight; m, months.

concentrations of IL-18 (Figure 3F) and lower concentrations of IL-18–binding protein (IL-18BP) (Figure 3H) were evident in alveolar macrophages after 2 months of SHS exposure (Figures 3E and 3G, respectively).

SHS exposure resulted in a significant increase in IL-18 protein (Figure 3I) and mRNA (Figure 3J) concentrations in the BALF macrophages. Concentrations of chemokine (C-C motif) ligand 5 (CCL5) in BALF (Figure 3K) were also significantly increased after 2 months of SHS exposure.

The proinflammatory nature of IL-18 was confirmed by exposing IL-18 KO mice and wild-type control mice to heat-inactivated *Staphylococcus epidermidis*. The IL-18 KO mice showed significantly fewer inflammatory infiltrates 20 hours after a single intratracheal instillation of *S. epidermidis* than did wild-type control mice (Figure E4).

IL-18 Concentrations in BALF from Patients with COPD

The ELISA technique was used to examine IL-18 concentrations in the BALF of patients with COPD and healthy age-matched control subjects. The patient demographics are presented in Table E1 in the online supplement. As shown in Figure E5A, a trend toward increased concentrations of IL-18 in BALF from current smokers (control subjects as well as patients with COPD) was evident. However, because of the small sample size, this trend did not reach statistical significance. Interestingly, increased IL-18 concentrations were detected in the BALF of active smokers from the control and COPD groups. We also observed a tendency toward a negative correlation between IL-18 concentrations in BALF and the percent predicted forced expiratory volume in 1 second (FEV_1) (Figure E5B).

IL-18 Affects VEGFR1 and VEGFR2 Expression, Induces Endothelial Cell Death, and Vascular Permeability

The treatment of RPMVECs *in vitro* with recombinant IL-18 (rIL-18) significantly down-regulated VEGF receptor–1 (VEGFR1) and VEGFR2 expression (Figures 4A and 4C). The quantitative analysis of Western blots is presented in Figure 4B (VEGFR1 expression) and Figure 4D (VEGFR2 expression). Furthermore, IL-18 induced RPMVEC death, as demonstrated by immunofluorescent staining for annexin V and active cleaved caspase-3. Cells were treated without IL-18 (Figure 4E) or with IL-18 (Figure 4F), and were stained with annexin V or active cleaved caspase-3 (no treatment, Figure 4G; IL-18 treatment, Figure 4H).

Treatment with rIL-18 or CSE also affected endothelial monolayer integrity. As determined by an Evans blue assay (Figure 5A), IL-18 and CSE treatment significantly increased endothelial

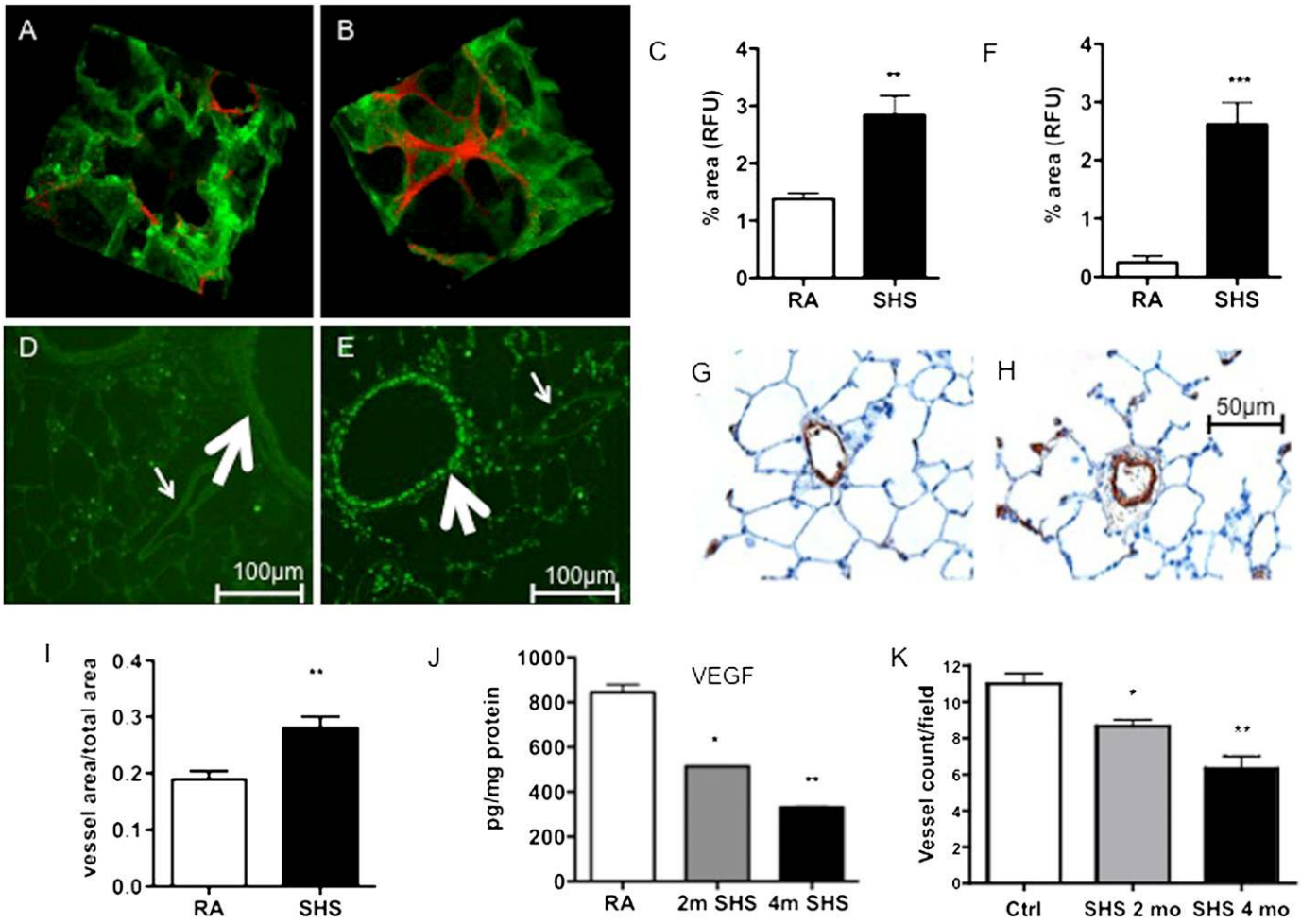

Figure 2. SHS exposure induced lung-tissue remodeling and cell death. (*A* and *B*) Paraformaldehyde-fixed, agarose-inflated 5-μm lung slices were imaged with nonlinear second-harmonic generation (SHG) microscopy. The acquisition of three-dimensional images was performed using a 5 × 5 tiling procedure. The autofluorescence of elastin (*green*) and the SHG signal of collagen (*red*) were determined in RA-exposed control rat lungs (*A*) and SHS-exposed lungs (*B*). (*C*) The quantitative analysis of collagen deposition was performed using Image J software (National Institutes of Health, Bethesda, MD). Cell death was determined by the TUNEL staining of RA-exposed rat lungs (*D*) and SHS-exposed lungs (*E*). *Thick arrows* indicate bronchioles, and *thin arrows* show the vasculature. (*F*) The quantification of terminal deoxynucleotidyl transferase dUTP nick end labeling (TUNEL) staining was performed using Image J software. Statistical analysis was performed using GraphPad Prism (San Diego, CA) and the Student *t* test. (*G*) Vascular endothelial growth factor (VEGF) protein concentrations in RA-exposed control rat lung tissue and in 2-month and 4-month SHS-exposed rat lung tissue extracts were measured by a Luminex assay (BioRad, Hercules, CA). Immunohistochemical staining for α–smooth muscle actin was performed on RA-exposed (*H*) and 2-month SHS-exposed (*I*) rat lung sections. (*J*) Pulmonary blood vessel thickness was measured using the Photoshop program (Adobe, San Jose, CA), and was expressed as a ratio of vessel wall area over total vessel area. Vessels of equal diameter were assessed. Three slides per group with 10 vessels per slide were evaluated. (*K*) Blood vessel counts per field. Vessel counting was performed on α–smooth muscle actin–stained slides at ×200 magnification (three slides per group, three fields per slide). $^*P < 0.05$. $^{**}P \leq 0.01$. $^{***}P \leq 0.001$. Ctrl, control; RFU, relative fluorescence units.

monolayer permeability. In addition, IL-18 and CSE induced inflammatory cell migration, as monitored by carboxyfluorescein succinimidyl ester–labeled rAM migration via the endothelial cell monolayer. The fluorescence intensity data measured in the lower part of the Boyden chamber are presented in Figure 5B.

DISCUSSION

SHS exposure can be a serious health hazard for nonsmokers. However, a 2006 report by the United States Surgeon General concluded that the evidence linking SHS and COPD is only suggestive (www.surgeongeneral.gov/library/secondhandsmoke), and not sufficient to infer a causal relationship. The conclusion of that report was primarily drawn from the epidemiologic evidence (17–24), which did not establish a biological link. Here we have challenged this conclusion by providing evidence that SHS exposure causes phenotypic changes consistent with emphysema. Rats exposed to SHS at the concentrations that reproduce smoke concentrations recorded at the casinos of North America developed significant emphysema after 2 months of exposure. The enlargement of alveolar airspaces was progressive (Figures 1B and 1C). Usually at least 6 months of smoke exposure are required to induce emphysema in mice (25). Moreover, rats are quite sensitive to smoke exposure, and initially could not tolerate such high concentrations of TPM. They had to be acclimated to 50% concentrations of the target dose during the first week of exposure, and to 75% during the second week of exposure. Lee and colleagues (26) reported emphysematous changes in rat lungs after 4 months of mainstream cigarette smoke exposure. This suggests that SHS exposure is even more harmful than mainstream smoke because emphysematous changes are present after 2 months of exposure, and therefore

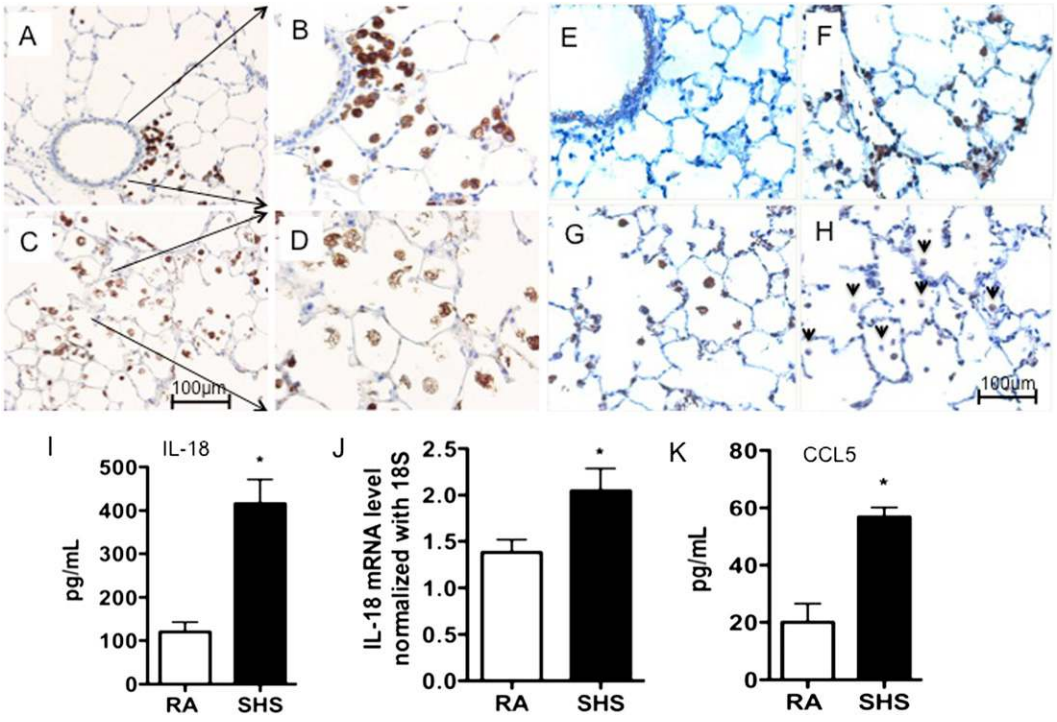

Figure 3. Immunohistochemical staining of rat lungs for macrophage marker CD68, IL-18, and IL-18–binding protein (IL-18BP). CD68 staining was performed in RA-exposed control rat lungs (*A* and *B*) and 2-month SHS-exposed rat lungs (*C* and *D*). Staining was undertaken for IL-18 in RA-exposed rat lungs (*E*) versus 2-month SHS-exposed rat lungs (*F*). Staining was also performed for IL-18BP in alveolar macrophages of RA-exposed rat lungs (*G*) and 2-month SHS-exposed (*H*) rat lungs. Concentrations of IL-18 cytokine (*I*) and IL-18 mRNA (*J*) were determined in bronchoalveolar lavage fluid (BALF) cells from RA-exposed and 2-month SHS-exposed rats (*J*). (*K*) Protein concentrations of chemokine (C-C motif) ligand 5 (CCL5) were determined in BALF of RA-exposed and 2-month SHS-exposed rats. *$P < 0.05$. *Arrows* in *A* and *C* indicate the enlarged areas shown in *B* and *D*.

our rat model of progressive emphysema may be of utility in intervention studies.

Exposure to SHS resulted in significant weight loss that correlated with reduced concentrations of leptin (Figure E1 in the online supplement). This weight loss most likely reflects increased concentrations of free fatty acids and catecholamines in the plasma (27). Low concentrations of leptin have also been implicated in smokers with COPD, and have been associated

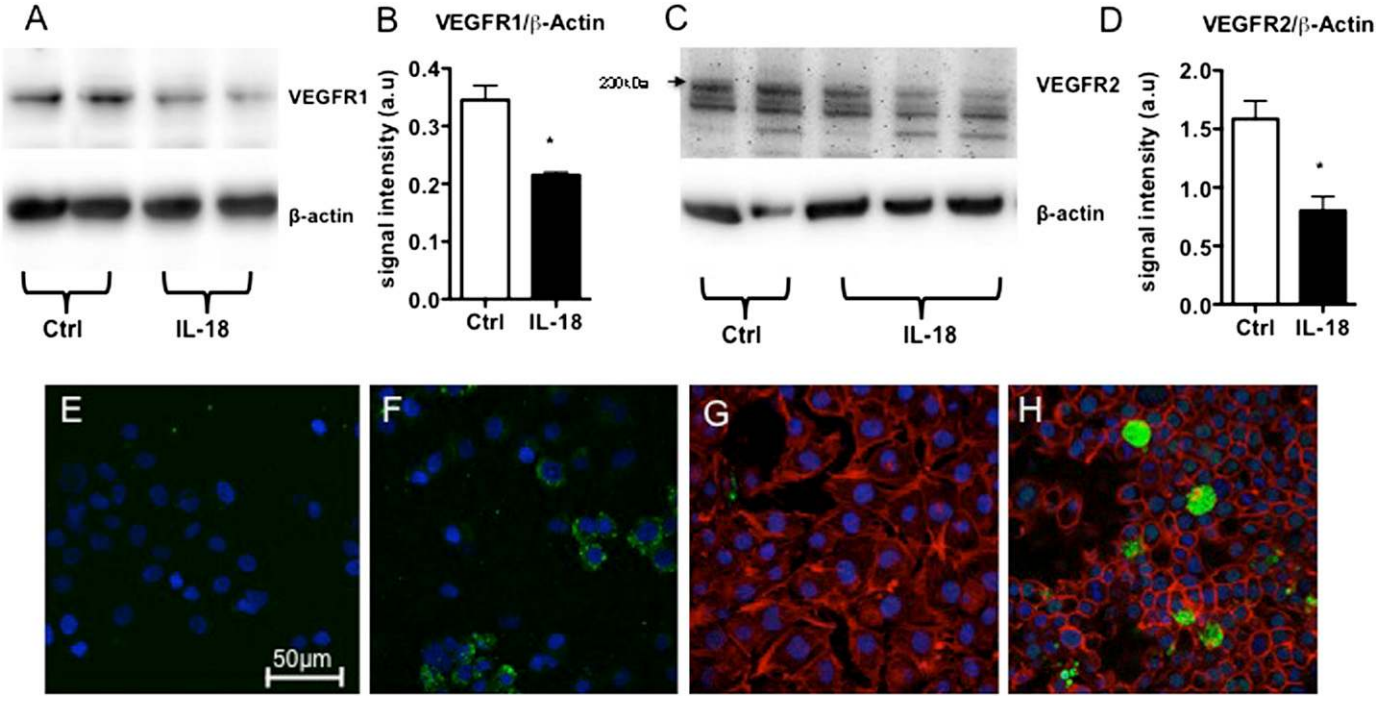

Figure 4. Western blot analysis of rat pulmonary microvascular endothelial cells (RPMVECs) untreated (Ctrl), or treated with 3% cigarette smoke extract (CSE) or rat recombinant IL-18 (100 ng/ml). The blots are representative of VEGF receptor–1 (VEGFR1) (*A*) and VEGFR2 (C). The three bands of VEGFR2 represent the mature, fully glycosylated form (230 kD), the intermediate, partly glycosylated form (200 kD), and the immature form (180 kD). The quantitative analysis of Western blots involved VEGFR1 (*B*) and the mature 230-kD (indicated with an *arrow*) form of VEGFR2 (*D*). IL-18–induced RPMVEC death was detected by immunofluorescent staining for annexin V and caspase-3. Annexin V staining was performed in control cells (*E*) and IL-18–treated RPMVECs (*F*). Caspase-3 staining was performed in control cells (*G*) and IL-18–treated RPMVECs (H). Annexin V and caspase-3 stained *green*, F-actin–rhodamine B phalloidin stained *red*, and DAPI stained *blue* for nuclei. a.u., arbitrary units. *$P < 0.05$. a.u., arbitrary units.

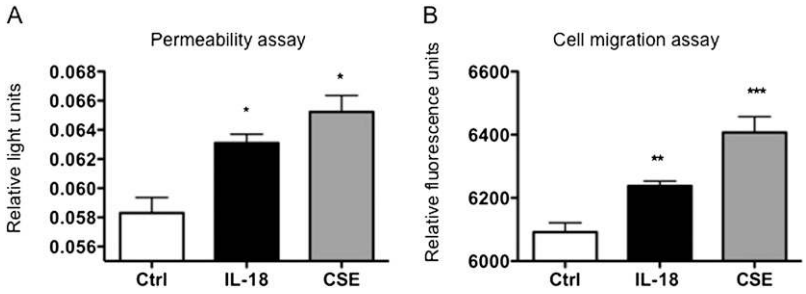

Figure 5. Permeability (*A*) and macrophage migration (*B*) assays. After serum starvation, RPMVEC monolayers were treated with IL-18 (100 ng/mL) or 10% CSE for 12 hours. (*A*) The relative light intensity of the albumin-bound Evans blue was determined by measuring absorbance at a wavelength of 620 nm. (*B*) Macrophage migration was assessed using carboxyfluorescein succinimidtl ester–labeled alveolar macrophages after 24 hours. The relative fluorescence intensity in the lower Boyden chamber was measured using a Victor 3 fluorescence plate reader (excitation at 488 nm; Perkin-Elmer, Waltham, MA). $*P < 0.05$. $**P \leq 0.01$. $***P \leq 0.001$.

with sexual dysfunction, impaired glucose tolerance, osteoporosis, and pulmonary infections (28). Moreover, chronic exposure to cigarette smoke is associated with weight loss because tobacco compounds stimulate the hypothalamus in an appetite-reducing manner (29) and affect leptin metabolism. Reduced leptin concentrations have been reported in healthy male smokers (30).

Rats exposed to SHS developed right ventricular hypertrophy (Figures 1E and 1F) and lung tissue remodeling that resulted in fewer blood vessels and a significant degree of muscularization of the remaining vessels, as demonstrated by α–smooth muscle actin staining (Figures 2G–2I), suggesting mild pulmonary hypertension. A retrospective study performed on 409 patients with endstage COPD/emphysema or α-1–antitrypsin deficiency found the incidence of pulmonary hypertension to be 36% (31). However, the association with smoking status was not examined. The development of pulmonary hypertension worsens the prognosis in patients with COPD. Recent data suggest that pulmonary hypertension may comprise a direct effect of tobacco smoke on intrapulmonary vessels, causing an abnormal production of mediators that control vasoconstriction, vasodilatation, and vascular cell proliferation. This ultimately leads to aberrant vascular remodeling and physiology (32–36).

In our animal model, increased collagen (fibrosis) and aberrant elastin layers in the lung tissue were evident, as demonstrated using SHG microscopy (Figure 2B). SHG microscopy is highly sensitive for collagen, does not require any labeling, and allows for the detection of fine changes in tissue remodeling that are undetectable with conventional immunohistochemistry.

Moreover, the alveolar macrophages in SHS-exposed rat lungs exhibited a foamy phenotype with increased numbers of apoptotic cell accumulations. This implies decreased phagocytotic clearance and signaling, as previously reported (37, 38).

An impaired regulation of inflammatory signaling in COPD has been reported, based on the increased numbers of inflammatory cells and their cytokine signaling (39–41). In murine alveolar macrophages, cigarette smoke exposure attenuated cytokine production (42). SHS exposure resulted in a decrease of leptin concentrations in rat lungs (Figure 3L), as well as in the vast majority of cytokines tested using a multiplex array (Table E1 in the online supplement). At the same time, a significant increase in IL-18 concentrations in the BALF of SHS-exposed rats was evident (Figure 3I). The precursor for IL-18 is found weakly expressed in nearly all lung cells, and the expression of the mature active form is strongly enhanced in macrophages after lung injury (43, 44). SHS exposure may induce the caspase-1 activity necessary to release the active IL-18 from alveolar macrophages. The IL-18 precursor can be also cleaved by neutrophil protease-3 (45). However, no neutrophils were evident in the BALF of SHS-exposed rats.

Although IL-18 has been implicated in cigarette smoke–induced pulmonary responses and elevated concentrations of IL-18 have been reported in the plasma of patients with COPD (46–49), the mechanisms behind IL-18–mediated lung injury remain unclear. Decreased concentrations of IL-18 were found in the sputum of active smokers, with a positive correlation between IL-18 concentrations and the percent predicted FEV_1 in asthmatic smokers (50). Very recently, Kang and colleagues (51) used lung-specific, inducible IL-18 transgenic mice to show that IL-18 can induce emphysema and vascular remodeling. That study supports our findings in a rat model of SHS-induced emphysema, where increased concentrations of IL-18 contributed to lung destruction and the development of emphysema. Moreover, a significant increase of CCL5 in the BALF was evident after 2 months of SHS exposure, and CCL5 was previously shown to be increased in the sputum of patients with COPD (52).

IL-18 plays a role in cardiovascular disease (53), which is consistent with the observation of mild right ventricular hypertrophy after SHS exposure (Figures 1E and 1F). In the transgenic murine model, the overexpression of mature IL-18 in the lungs resulted in an increased production of IFN-γ, IL-5, and IL-13, chronic lung inflammation, and age-dependent emphysematous lung destruction (48). Here we show that IL-18–deficient mice are protected against the excessive inflammation caused by *S. epidermidis* infection, indicating an important role of this cytokine in the inflammatory response (Figure E3).

Studies have demonstrated in a murine model system that IL-18 receptor (IL-18R) signaling is involved in the pathogenesis of cigarette smoke–induced inflammation and emphysema (47, 54). In fact, IL-18R null mice were partly protected from cigarette smoke–induced emphysema. Recently, circulating concentrations of IL-18 in patients with COPD at Global Initiative on Obstructive Lung Disease (GOLD) Stages III and IV were reported to be significantly higher than in smokers and nonsmokers, suggesting that IL-18 may play a role in the pathogenesis of COPD (47, 49).

Our study shows for the first time the involvement of IL-18 in pulmonary endothelial cell death and the development of emphysema after SHS exposure.

The recombinant IL-18 or CSE induced microvascular endothelial cell death. Moreover, IL-18 down-regulated the expression of both VEGFR1 and VEGFR2 in RPMVECs. Earlier, we demonstrated that blocking VEGFR signaling with the VEGFR inhibitor SU5416 induces endothelial cell apoptosis and emphysema (7). SU5416 is known to block both VEGFR1 and VEGFR2. In fact, SU5416 demonstrates a higher affinity for VEGFR1 than for VEGFR2, suggesting that VEGFR1 may be the primary target of apoptosis induction in emphysema. Recently, pulmonary endothelial cells were reported to express higher concentrations of VEGFR1 than of VEGFR2 (55).

Our data on SHS-exposed rats suggest that IL-18–induced endothelial cell death occurs as a result of an inhibition of VEGFR signaling.

IL-18BP is a naturally occurring inhibitor of IL-18 activity and demonstrates higher affinity for IL-18 than for the receptor of IL-18 (56, 57). IL-18BP is known to decrease the severity of inflammation in response to injury, and an imbalance between concentrations of free IL-18 and IL-18BP affects the severity of some inflammatory diseases (58). An adoptive transfer of mesenchymal

stem cells derived from mice transgenic for overexpressing human IL-18BP improved myocardial function in rat models of myocardial ischemia (59). Here we show, for the first time, that SHS exposure decreased IL-18BP expression in alveolar macrophages (Figure 3H). Our data suggest a therapeutic potential for IL-18BP in COPD. The natural stimulant for IL-18BP production is IFN-γ (60). However, we found decreased concentrations of IFN-γ in the lung tissue and undetectable concentrations in the BALF after SHS exposure, which correlates with the decreased expression of IL-18BP in alveolar macrophages.

In conclusion, the present work and the research of others show that SHS exposure causes similarly deleterious effects in rat models. SHS impairs immune responses in the lung, and after 2 months of exposure, leads to measurable, progressive emphysema and right ventricular hypertrophy. SHS impairs the lung's first line of defense, namely, macrophage function, leading to increased secretions of the proinflammatory mediator IL-18 that mediates emphysematous lung destruction by inducing the apoptosis of microvascular endothelial cells via the downregulation of VEGFR1 and VEGFR2. Our study indicates that IL-18 as well as its binding protein may comprise potential targets for new therapies in COPD.

Author disclosures are available with the text of this article at www.atsjournals.org.

Acknowledgments: The authors thank Dr. Ivor Douglas for assisting with the Image J software tools and Dr. Rubin Tuder for assistance with lung quantification methods according to American Thoracic Society guidelines. The authors greatly appreciate help from Radu Moldovan and Gregory Glazner with SHG microscopy, and help from Danny Zipris with the Luminex machine. The authors also express their gratitude to Ruth Francesca for technical assistance with smoking, as well as to Aneta Gandjeva and Mario Perez for lung-volume measurements. Finally, the authors thank Dr. John Stewart and Dr. Marvin Schwartz for their critical reading of the manuscript.

References

1. Chung KF, Adcock IM. Multifaceted mechanisms in COPD: inflammation, immunity, and tissue repair and destruction. *Eur Respir J* 2008;31:1334–1356.
2. Yoshida T, Tuder RM. Pathobiology of cigarette smoke–induced chronic obstructive pulmonary disease. *Physiol Rev* 2007;87:1047–1082.
3. Eisner MD, Anthonisen N, Coultas D, Kuenzli N, Perez-Padilla R, Postma D, Romieu I, Silverman EK, Balmes JR. An official American Thoracic Society public policy statement: novel risk factors and the global burden of chronic obstructive pulmonary disease. *Am J Respir Crit Care Med* 2010;182:693–718.
4. Oberg M, Jaakkola MS, Woodward A, Peruga A, Pruss-Ustun A. Worldwide burden of disease from exposure to second-hand smoke: a retrospective analysis of data from 192 countries. *Lancet* 2010;377:139–146.
5. Taraseviciene-Stewart L, Voelkel NF. Molecular pathogenesis of emphysema. *J Clin Invest* 2008;118:394–402.
6. Nold-Petry CA, Nold MF, Nielsen JW, Bustamante A, Zepp JA, Storm KA, Hong JW, Kim SH, Dinarello CA. Increased cytokine production in interleukin-18 receptor alpha–deficient cells is associated with dysregulation of suppressors of cytokine signaling. *J Biol Chem* 2009; 284:25900–25911.
7. Kasahara Y, Tuder RM, Taraseviciene-Stewart L, Le Cras TD, Abman S, Hirth PK, Waltenberger J, Voelkel NF. Inhibition of VEGF receptors causes lung cell apoptosis and emphysema. *J Clin Invest* 2000;106:1311–1319.
8. Hsia CC, Hyde DM, Ochs M, Weibel ER. An official research policy statement of the American Thoracic Society/European Respiratory Society: standards for quantitative assessment of lung structure. *Am J Respir Crit Care Med* 2010;181:394–418.
9. Yoshida T, Mett I, Bhunia AK, Bowman J, Perez M, Zhang L, Gandjeva A, Zhen L, Chukwueke U, Mao T, *et al*. RTP801, a suppressor of mTor signaling, is an essential mediator of cigarette smoke–induced pulmonary injury and emphysema. *Nat Med* 2010;16:767–773.
10. Robbesom AA, Versteeg EM, Veerkamp JH, van Krieken JH, Bulten HJ, Smits HT, Willems LN, van Herwaarden CL, Dekhuijzen PN, van Kuppevelt TH. Morphological quantification of emphysema in small human lung specimens: comparison of methods and relation with clinical data. *Mod Pathol* 2003;16:1–7.
11. Knudsen L, Weibel ER, Gundersen HJ, Weinstein FV, Ochs M. Assessment of air space size characteristics by intercept (chord) measurement: an accurate and efficient stereological approach. *J Appl Physiol* 2010; 108:412–421.
12. Mitzner W, Fallica J, Bishai J. Anisotropic nature of mouse lung parenchyma. *Ann Biomed Eng* 2008;36:2111–2120.
13. Taraseviciene-Stewart L, Scerbavicius R, Choe KH, Moore M, Sullivan A, Nicolls MR, Fontenot AP, Tuder RM, Voelkel NF. An animal model of autoimmune emphysema. *Am J Respir Crit Care Med* 2005; 171:734–742.
14. Carp H, Janoff A. Possible mechanisms of emphysema in smokers: *in vitro* suppression of serum elastase–inhibitory capacity by fresh cigarette smoke and its prevention by antioxidants. *Am Rev Respir Dis* 1978;118:617–621.
15. Repace JL, Jiang RT, Acevedo-Bolton V, Cheng KC, Klepeis NE, Ott WR, Hildemann LM. Fine particle air pollution and secondhand smoke exposures and risks inside 66 US casinos. *Environ Res* 2011; 111:473–484.
16. (CDC) CfDCaP. Indoor air quality at nine large-hub airports with and without designated smoking areas: United States, October–November 2012. *MMWR Morb Mortal Wkly Rep* 2012;61:948–951.
17. Robbins AS, Abbey DE, Lebowitz MD. Passive smoking and chronic respiratory disease symptoms in non-smoking adults. *Int J Epidemiol* 1993;22:809–817.
18. Dayal HH, Khuder S, Sharrar R, Trieff N. Passive smoking in obstructive respiratory disease in an industrialized urban population. *Environ Res* 1994;65:161–171.
19. Leuenberger P, Schwartz J, Ackermann-Liebrich U, Blaser K, Bolognini G, Bongard JP, Brandli O, Braun P, Bron C, Brutsche M, *et al*. Passive smoking exposure in adults and chronic respiratory symptoms (SAPALDIA Study): Swiss Study on Air Pollution and Lung Diseases in Adults, SAPALDIA Team. *Am J Respir Crit Care Med* 1994;150: 1222–1228.
20. Piitulainen E, Tornling G, Eriksson S. Environmental correlates of impaired lung function in non-smokers with severe alpha 1–antitrypsin deficiency (PIZZ). *Thorax* 1998;53:939–943.
21. Kalandidi A, Trichopoulos D, Hatzakis A, Tzannes S, Saracci R. Passive smoking and chronic obstructive lung disease. *Lancet* 1987;2:1325–1326.
22. Hirayama T. Non-smoking wives of heavy smokers have a higher risk of lung cancer: a study from Japan. *Br Med J (Clin Res Ed)* 1981;282:183–185.
23. Sandler DP, Comstock GW, Helsing KJ, Shore DL. Deaths from all causes in non-smokers who lived with smokers. *Am J Public Health* 1989;79:163–167.
24. Berglund DJ, Abbey DE, Lebowitz MD, Knutsen SF, McDonnell WF. Respiratory symptoms and pulmonary function in an elderly nonsmoking population. *Chest* 1999;115:49–59.
25. Takubo Y, Guerassimov A, Ghezzo H, Triantafillopoulos A, Bates JH, Hoidal JR, Cosio MG. Alpha1-antitrypsin determines the pattern of emphysema and function in tobacco smoke–exposed mice: parallels with human disease. *Am J Respir Crit Care Med* 2002;166:1596–1603.
26. Lee JH, Lee DS, Kim EK, Choe KH, Oh YM, Shim TS, Kim SE, Lee YS, Lee SD. Simvastatin inhibits cigarette smoking–induced emphysema and pulmonary hypertension in rat lungs. *Am J Respir Crit Care Med* 2005;172:987–993.
27. Reseland JE, Mundal HH, Hollung K, Haugen F, Zahid N, Anderssen SA, Drevon CA. Cigarette smoking may reduce plasma leptin concentration via catecholamines. *Prostaglandins Leukot Essent Fatty Acids* 2005;73:43–49.
28. Malli F, Papaioannou AI, Gourgoulianis KI, Daniil Z. The role of leptin in the respiratory system: an overview. *Respir Res* 2010;11:152.
29. Chen H, Hansen MJ, Jones JE, Vlahos R, Bozinovski S, Anderson GP, Morris MJ. Cigarette smoke exposure reprograms the hypothalamic neuropeptide Y axis to promote weight loss. *Am J Respir Crit Care Med* 2006;173:1248–1254.
30. Koc B, Bulucu F, Karadurmus N, Sahin M. Lower leptin levels in young nonobese male smokers than non-smokers. *Ups J Med Sci* 2009;114:165–169.
31. Andersen KH, Iversen M, Kjaergaard J, Mortensen J, Nielsen-Kudsk JE, Bendstrup E, Videbaek R, Carlsen J. Prevalence, predictors, and survival in pulmonary hypertension related to end-stage chronic obstructive pulmonary disease. *J Heart Lung Transplant* 2012;31:373–380.

32. Wright JL, Levy RD, Churg A. Pulmonary hypertension in chronic obstructive pulmonary disease: current theories of pathogenesis and their implications for treatment. *Thorax* 2005;60:605–609.
33. Orr R, Smith LJ, Cuttica MJ. Pulmonary hypertension in advanced chronic obstructive pulmonary disease. *Curr Opin Pulm Med* 2012;18: 138–143.
34. Voelkel NF, Gomez-Arroyo J, Mizuno S. COPD/emphysema: the vascular story. *Pulm Circ* 2012;1:320–326.
35. Chaouat A, Naeije R, Weitzenblum E. Pulmonary hypertension in COPD. *Eur Respir J* 2008;32:1371–1385.
36. Andersen KH, Iversen M, Kjaergaard J, Mortensen J, Nielsen-Kudsk JE, Bendstrup E, Videbaek R, Carlsen J. Prevalence, predictors, and survival in pulmonary hypertension related to end-stage chronic obstructive pulmonary disease. *J Heart Lung Transplant* 2012;31:373–380.
37. Renda T, Baraldo S, Pelaia G, Bazzan E, Turato G, Papi A, Maestrelli P, Maselli R, Vatrella A, Fabbri LM, *et al*. Increased activation of p38 MAPK in COPD. *Eur Respir J* 2008;31:62–69.
38. Richens TR, Linderman DJ, Horstmann SA, Lambert C, Xiao YQ, Keith RL, Boe DM, Morimoto K, Bowler RP, Day BJ, *et al*. Cigarette smoke impairs clearance of apoptotic cells through oxidant-dependent activation of RhoA. *Am J Respir Crit Care Med* 2009;179:1011–1021.
39. Snoeck-Stroband JB, Postma DS, Lapperre TS, Gosman MM, Thiadens HA, Kauffman HF, Sont JK, Jansen DF, Sterk PJ. Airway inflammation contributes to health status in COPD: a cross-sectional study. *Respir Res* 2006;7:140.
40. Sinden NJ, Stockley RA. Systemic inflammation and comorbidity in COPD: a result of "overspill" of inflammatory mediators from the lungs? Review of the evidence. *Thorax* 2010;65:930–936.
41. Cornwell WD, Kim V, Song C, Rogers TJ. Pathogenesis of inflammation and repair in advanced COPD. *Semin Respir Crit Care Med* 2010;31: 257–266.
42. Gaschler GJ, Zavitz CC, Bauer CM, Skrtic M, Lindahl M, Robbins CS, Chen B, Stampfli MR. Cigarette smoke exposure attenuates cytokine production by mouse alveolar macrophages. *Am J Respir Cell Mol Biol* 2008;38:218–226.
43. Dinarello CA. Interleukin 1 and interleukin 18 as mediators of inflammation and the aging process. *Am J Clin Nutr* 2006;83:447S–455S.
44. Jordan JA, Guo RF, Yun EC, Sarma V, Warner RL, Crouch LD, Senaldi G, Ulich TR, Ward PA. Role of IL-18 in acute lung inflammation. *J Immunol* 2001;167:7060–7068.
45. Sugawara S, Uehara A, Nochi T, Yamaguchi T, Ueda H, Sugiyama A, Hanzawa K, Kumagai K, Okamura H, Takada H. Neutrophil proteinase 3–mediated induction of bioactive IL-18 secretion by human oral epithelial cells. *J Immunol* 2001;167:6568–6575.
46. Petersen AM, Penkowa M, Iversen M, Frydelund-Larsen L, Andersen JL, Mortensen J, Lange P, Pedersen BK. Elevated levels of IL-18 in plasma and skeletal muscle in chronic obstructive pulmonary disease. *Lung* 2007;185:161–171.
47. Kang MJ, Homer RJ, Gallo A, Lee CG, Crothers KA, Cho SJ, Rochester C, Cain H, Chupp G, Yoon HJ, *et al*. IL-18 is induced and IL-18 receptor alpha plays a critical role in the pathogenesis of cigarette smoke–induced pulmonary emphysema and inflammation. *J Immunol* 2007;178:1948–1959.
48. Hoshino T, Kato S, Oka N, Imaoka H, Kinoshita T, Takei S, Kitasato Y, Kawayama T, Imaizumi T, Yamada K, *et al*. Pulmonary inflammation and emphysema: role of the cytokines IL-18 and IL-13. *Am J Respir Crit Care Med* 2007;176:49–62.
49. Imaoka H, Hoshino T, Takei S, Kinoshita T, Okamoto M, Kawayama T, Kato S, Iwasaki H, Watanabe K, Aizawa H. Interleukin-18 production and pulmonary function in COPD. *Eur Respir J* 2008;31:287–297.
50. Rovina N, Dima E, Gerassimou C, Kollintza A, Gratziou C, Roussos C. IL-18 in induced sputum and airway hyperresponsiveness in mild asthmatics: effect of smoking. *Respir Med* 2009;103:1919–1925.
51. Kang MJ, Choi JM, Kim BH, Lee CM, Cho WK, Choe G, Kim DH, Lee CG, Elias JA. IL-18 induces emphysema, and airway and vascular remodeling via IFN-gamma, IL-17A and IL-13. *Am J Respir Crit Care Med* 2012;185:1205–1217.
52. Di Stefano A, Caramori G, Gnemmi I, Contoli M, Bristot L, Capelli A, Ricciardolo FL, Magno F, D'Anna SE, Zanini A, *et al*. Association of increased CCL5 and CXCL7 chemokine expression with neutrophil activation in severe stable copd. *Thorax* 2009;64:968–975.
53. Sims JE, Smith DE. The IL-1 family: regulators of immunity. *Nat Rev Immunol* 2010;10:89–102.
54. Kang MJ, Lee CG, Lee JY, Dela Cruz CS, Chen ZJ, Enelow R, Elias JA. Cigarette smoke selectively enhances viral PAMP– and virus-induced pulmonary innate immune and remodeling responses in mice. *J Clin Invest* 2008;118:2771–2784.
55. Ma B, Dela Cruz CS, Hartl D, Kang MJ, Takyar S, Homer RJ, Lee CG, Elias JA. Rig-like helicase innate immunity inhibits vascular endothelial growth factor tissue responses via a Type I IFN-dependent mechanism. *Am J Respir Crit Care Med* 2011;183:1322–1335.
56. Novick D, Kim SH, Fantuzzi G, Reznikov LL, Dinarello CA, Rubinstein M. Interleukin-18 binding protein: a novel modulator of the Th1 cytokine response. *Immunity* 1999;10:127–136.
57. Kim SH, Eisenstein M, Reznikov L, Fantuzzi G, Novick D, Rubinstein M, Dinarello CA. Structural requirements of six naturally occurring isoforms of the IL-18 binding protein to inhibit IL-18. *Proc Natl Acad Sci USA* 2000;97:1190–1195.
58. Mazodier K, Marin V, Novick D, Farnarier C, Robitail S, Schleinitz N, Veit V, Paul P, Rubinstein M, Dinarello CA, *et al*. Severe imbalance of IL-18/IL-18BP in patients with secondary hemophagocytic syndrome. *Blood* 2005;106:3483–3489.
59. Wang M, Tan J, Wang Y, Meldrum KK, Dinarello CA, Meldrum DR. IL-18 binding protein-expressing mesenchymal stem cells improve myocardial protection after ischemia or infarction. *Proc Natl Acad Sci USA* 2009;106:17499–17504.
60. Hurgin V, Novick D, Werman A, Dinarello CA, Rubinstein M. Antiviral and immunoregulatory activities of IFN-gamma depend on constitutively expressed IL-1alpha. *Proc Natl Acad Sci USA* 2007;104:5044–5049.